Reprinted from the American Ceramics Society Bulletin, Vol. 63, No. 9-10 September-October 1980


# Flaw Characteristics in Dynamic Fatigue: The Influence of Residual Contact Stresses

D. B. MARSHALL*,* and B. R. LAWN*

Department of Applied Physics, School of Physics, University of New South Wales, Kensington, New South Wales 2033, Australia

**The effect of residual contact stresses on the dynamic fatigue response of surfaces containing indentation-induced flaws is studied. Indentation fracture mechanics is used to analyze the growth of well-defined "median/radial" cracks in combined residual (elastic/plastic) contact and applied (uniform) tensile fields, and thence to determine strength characteristics. In this way a general formulation is obtained for the fatigue strength at constant stress rate. Experimental confirmation of the essential predictions of the theory is obtained from strength tests on Vickers-indented soda-lime glass disks in water environment. It is thereby implied that residual stresses can have a significant deleterious influence on the fatigue behavior of any brittle solid whose controlling flaws have a contact history. Such effects need to be considered in the design of structural ceramics, most notably where fracture-mechanics calibrations of crack-velocity parameters are used for lifetime predictions.**

## I. Introduction

CERAMICS are susceptible to stress-enhanced crack growth in the presence of certain chemical environments, notably water.[1] Consequently, the use of these materials as structural components requires due allowance to be made for "fatigue" effects in design specifications. Quantities such as "minimum lifetime" at constant applied stress ("static" fatigue) or "homologous strength" at constant stress *rate* ("dynamic" fatigue) now form an important part of the characterization of brittle fracture.[2-6]

Analysis of fatigue properties generally begins with the tacit assumption that failure is preceded by the subcritical extension of well-defined "Griffith" flaws. An appropriate crack-velocity/stress-intensity-factor function for the given material/environment system is then invoked, from which the flaw response may be evaluated. This function is invariably obtained by empirical data fits to results from large-scale fracture specimens. While the use of crack-velocity data in predicting fatigue characteristics has met with widespread success, several studies have indicated that some important differences may exist between macroscopic-crack and microscopic-flaw behavior under ostensibly identical test conditions[7-11]; discrepancies in the values of the exponent $n$ in power-law crack-velocity functions are the clearest manifestation of this conclusion. Such differences are particularly pertinent to applications in which short-term fracture mechanics data are used to predict long-term strengths.

Recent investigations into the nature of indentation crack patterns in silicate glasses and other ceramics[12-18] provide some insight into the mechanics of fracture at a level between those of flaw and large-scale crack. The case of special interest is that of elastic/plastic contact, produced in sharp-point indentation, in which irreversible processes play a major role in the crack evolution. Most significantly, the irreversible component of the field gives rise to a residual opening force on the newly formed crack. This residual force contributes to the net driving force on the crack system during subsequent stressing, as in a strength test; typically, a measured strength ≈30 to 40% lower than that predicted from crack dimensions and known stress intensity factor alone is obtained under conditions of equilibrium fracture.[19]

In this study the influence of residual contact stresses on crack growth under nonequilibrium conditions is examined. In particular, the dynamic fatigue characteristics are determined for a convenient model "flaw" system, Vickers-indented soda-lime glass surfaces in a water environment. The residual-stress effect is demonstrated most clearly by comparing strength data for surfaces in the as-indented state with those for surfaces annealed between the contact- and failure-test stages. A theoretical analysis of the results, based on indentation fracture mechanics, provides the necessary formalism for quantifying the residual term. Implications concerning the prospective response of surfaces containing general handling flaws are discussed.

## II. Incorporation of Residual-Stress Terms into Dynamic Fatigue Formulation

### *(1) Stress Intensity Factor for Indentation/Strength Model*

Figure 1 shows the model flaw system under consideration. In the indentation stage, Fig. 1(*A*), a well-defined crack system is produced, with characteristic dimension $c$ determined by the peak load

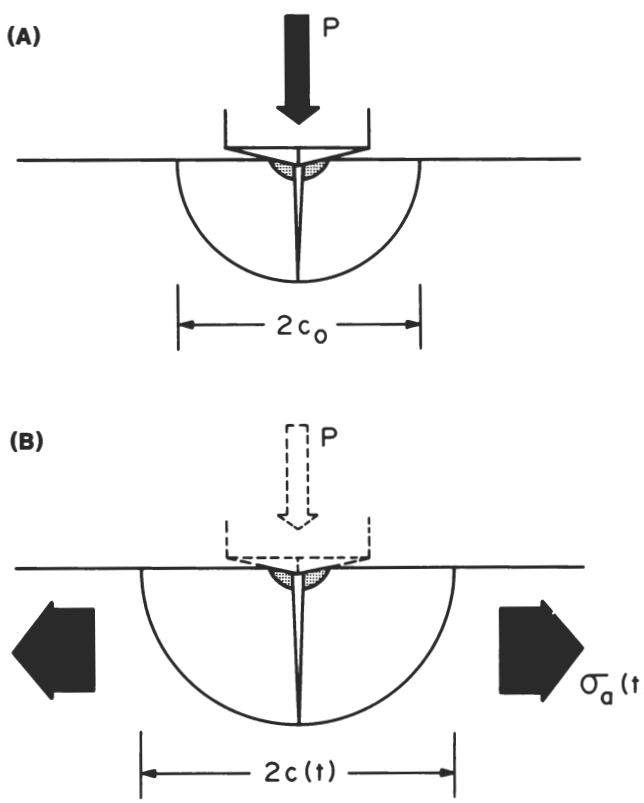


**Fig. 1.** Indentation/strength model system. (*A*) Vickers indenter, peak load $P$, generates median/radial crack, characteristic dimension $c$ (value $c_0$ at completion of contact cycle, with further postindentation, subcritical extension to $c_0'$ if exposed to moisture). (*B*) Tensile field $\sigma_a$, in combination with residual ("ghost") contact field, drives crack system to failure.

Received December 10, 1979; revised copy received March 17, 1980.
Supported by a grant from the Australian Department of Defense.
*Member, the American Ceramic Society.
*Now with the Materials and Molecular Research Division, Lawrence Berkeley Laboratory, University of California, Berkeley, California 94720.

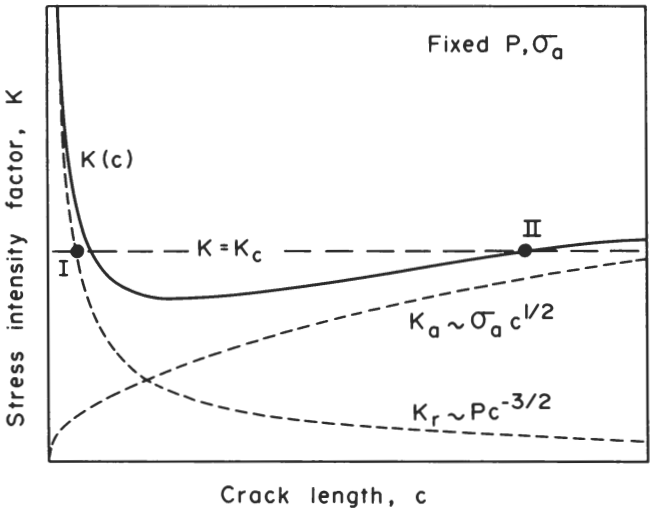


**Fig. 2.** Stress intensity factor for indentation flaw with residual stress. Point I represents (stable) equilibrium configuration at completion of indentation cycle; II represents (unstable) configuration at failure in subsequent strength test.

$P$.[12] The crack geometry depends to some extent on that of the indenter; here we consider the "median/radial" system[18] produced in Vickers indentation, consisting of two orthogonal, near-semicircular surface cracks intersecting along the load axis. A second set of cracks, the "lateral" system[12] (not indicated in Fig. 1), spreads sideways beneath the indentation surface; it remains passive in any subsequent tensile loading of the type depicted in Fig. 1(*B*)[17] and is accordingly disregarded in the theoretical formulation (although due allowance for secondary, radial/lateral interaction effects in the fracture mechanics will be shown to be necessary in some experimental determinations (Section III)). By virtue of the elastic/plastic nature of the point contact field, the median/radial crack system experiences a substantial residual opening force, which may be quantified by the stress intensity factor

$$K_r = \chi_r P/c^{3/2} \tag{1}$$

where $\chi_r$ is a dimensionless indenter/specimen constant.[17,18] The central importance of the residual field is apparent from the radial (surface-trace) crack response in glass: for indentation in inert (moisture-free) environments, the radial cracks grow almost exclusively during the unloading half-cycle, to some final equilibrium ($K_r = K_c$) size $c_0$[18]; if then the glass surface is exposed to moisture, the unloaded cracks expand subcritically ($K_r < K_c$) to some nonequilibrium size $c_0' > c_0$.

In the tensile strength-test stage, Fig. 1(*B*), an applied stress $\sigma_a$ augments the residual driving force. The appropriate stress intensity factor for this second term is of the standard form

$$K_a = \sigma_a(\pi\Omega c)^{1/2} \tag{2}$$

where $\Omega$ is a crack-geometry parameter. Thus the crack system is subject to a *net* stress intensity factor

$$K = \chi_r P/c^{3/2} + \sigma_a(\pi\Omega c)^{1/2} \qquad (c \geqslant c_0') \tag{3}$$

The function $K = K(c)$ is plotted in Fig. 2. Note that the influence of the residual component is greatest at small $c$, reflecting the localized nature of the responsible contact deformation processes. Fatigue characteristics may now be determined from Eq. (3) for any time-dependent stress $\sigma_a(t)$, once a suitable crack-velocity function is specified.

Before investigating fatigue characteristics, however, it is useful to derive relations for the strength under conditions of equilibrium fracture.

### (2) *Equilibrium Strength Relations*

To take the indentation crack system in Fig. 1(*A*) to failure in Fig. 1(*B*) under ideal equilibrium conditions, one must proceed from the initial stable configuration I in Fig. 2 ($dK/dc < 0$) to the unstable configuration II ($dK/dc > 0$) such that $K = K_c$ remains satisfied at all intervening points. Thus, as $\sigma_a$ increases from zero to its critical value the crack undergoes a stage of precursor stable growth.[17] This is shown formally by inserting $K = K_c$ into Eq. (3) to obtain the stress/equilibrium-crack relation

$$\sigma_a = [K_c/(\pi\Omega c)^{1/2}][1 - \chi_r P/K_c c^{3/2}] \tag{4}$$

This function has a maximum ($d\sigma_a/dc = 0$) at

$$\sigma_m = 3K_c/4(\pi\Omega c_m)^{1/2} \tag{5a}$$

$$c_m = (4\chi_r P/K_c)^{2/3} \tag{5b}$$

For $c < c_m$ the crack is stable ($d\sigma_a/dc > 0$), for $c > c_m$ it is unstable ($d\sigma_a/dc < 0$); the condition for failure is that the system attain a configuration on the unstable branch of the $\sigma_a(c)$ curve.[17]

The equilibrium strength relation for any given indentation situation will then depend on the size of the initial radial crack relative to the value $c_m$. In the present context there are two cases of special interest. The first corresponds to the limit $\chi_r = 0$, i.e. indentations free of residual stress. This gives $c_m = 0$ in Eq. (5*b*), so the function $\sigma_a(c)$ has only an unstable branch. Failure thus occurs spontaneously at $\sigma_a = \sigma_i^0$, $c = c_0'$; Eq. (4) yields the appropriate inert, residual-stress-free strength

$$\sigma_i^0 = K_c/(\pi\Omega c_0')^{1/2} \qquad (\chi_r = 0) \tag{6}$$

It must be stressed that it is the crack size $c_0'$ immediately prior to strength testing, not the value $c_0 (\leqslant c_0')$ immediately after indentation, which is pertinent here. The second case of interest is that in which residual stresses are present, $\chi_r > 0$, such that $c_0' < c_m$. Then, since the point $(\sigma_a, c_0')$ falls on the stable branch of the $\sigma_a(c)$ function, failure can occur only if the crack is made to grow stably to $c = c_m$ by increasing the stress to $\sigma_a = \sigma_m = \sigma_i^r$; Eq. (5) accordingly gives the inert, residual-stress-sensitive strength

$$\sigma_i^r = [27K_c^4/256\chi_r(\pi\Omega)^{3/2}P]^{1/3} \qquad (\chi_r > 0) \tag{7}$$

Because of the existence of this "energy barrier" to failure, the strength is now no longer dependent on initial crack size $c_0'$, provided the requirement $c_0' < c_m$ is not violated.

### (3) *Dynamic Fatigue Relations*

Under conditions of nonequilibrium fracture, the crack growth from configurations I to II in Fig. 2 proceeds along a subcritical path $K < K_c$ in accordance with some appropriate crack-velocity function $v(K)$. The velocity function used most widely in fatigue analysis of well-defined crack systems is of the form

$$v = v_0(K/K_c)^n \qquad (K < K_c) \tag{8}$$

where $v_0$ and $n$ are constants for a given material/environment system. Equations (3) and (8) may be combined to obtain a differential equation for crack size in terms of time; for dynamic fatigue, where the applied stress increases at a constant rate $\dot{\sigma}_a$, i.e. $\sigma_a = \dot{\sigma}_a t$, the differential equation is

$$\dot{c}/v_0 = \{[\chi_r/K_c]P/c^{3/2} + [(\pi\Omega)^{1/2}/K_c]\dot{\sigma}_a c^{1/2} t\}^n \tag{9}$$

The aim in general dynamic fatigue analysis is to obtain the value of $\sigma_a$ at failure as a function of $\dot{\sigma}_a$; in terms of Eq. (9) the problem reduces to solving for the time $t_f$ to take the crack from its initial size ($c_0'$) to its final size (solution of Eq. (3) at $K = K_c$, $dK/dc > 0$ branch) in the subcritical region.

An analytical evaluation of Eq. (9) is possible only in the limits of either the first or the second term within the brace becoming zero. The second case, corresponding to $\dot{\sigma}_a = 0$, produces a trivial solution, in that the time-to-failure is infinite. (The solution could be used to determine the extent of crack growth, $c_0 \rightarrow c_0'$, that would occur between indentation and strength testing; experimentally, however, it is simpler to measure $c_0'$ directly immediately prior to application of the tensile stress.) The other case, corresponding to $\chi_r = 0$, is not trivial; it has the standard solution

$$\sigma^0 \approx B\dot{\sigma}_a^{1/(n+1)} \qquad (\chi_r = 0) \tag{10}$$

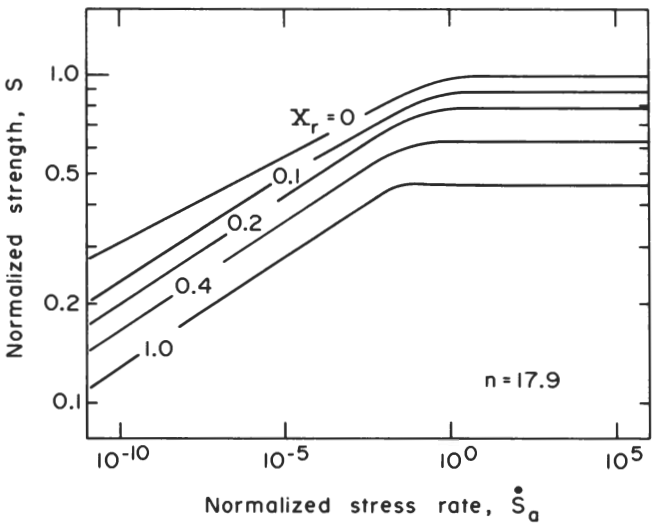


**Fig. 3.** Normalized dynamic fatigue curves for specimens containing indentation flaws with residual stress. Computed for specified $n$ and selected residual-stress parameters within range $0 \leq X_r \leq 1$.

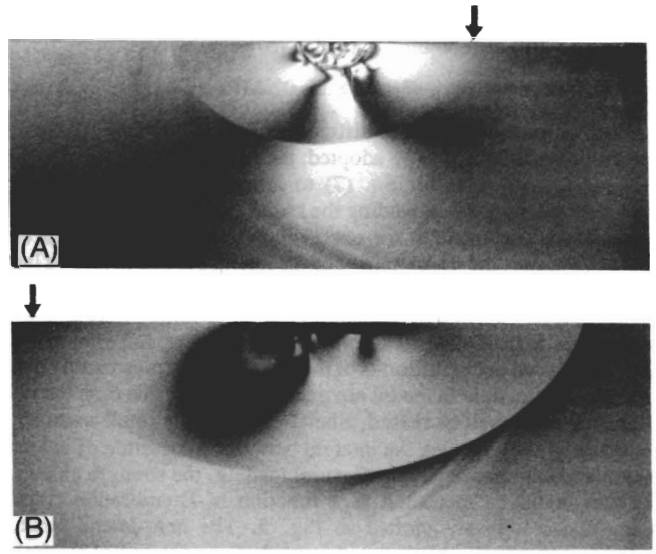


**Fig. 4.** Fracture surfaces of soda-lime glass disks broken in water, showing extended region of subcritical crack growth about indentation flaw. Indentation load $P = 5$ N, applied stress rate $\dot{\sigma}_a = 0.15$ MPa·s$^{-1}$. (*A*) Specimen annealed after indentation, failure stress $\sigma^0 = 62$ MPa; (*B*) specimen as-indented, failure stress $\sigma^r = 44$ MPa. Width of field 1.00 mm; arrows designate failure origins (faint surface markings beyond well-defined crack boundary tend to center on these origins).

in the strength region $\sigma^0 < \sigma_i^0$, where $B = \{[2(n+1)/(n-2)][K_c/(\pi\Omega)^{1/2}]^n / c_0'^{n/2-1} v_0\}^{1/(n+1)}$.

In general, Eq. (9) must be solved by numerical integration. It is convenient to rewrite the differential equation in normalized form by introducing the reduced variables $C = c/c_0'$, $T = tv_0/c_0'$, $X_r = \chi_r P/K_c c_0'^{3/2}$, $\dot{S}_a = \sigma_a(\pi\Omega c_0')^{1/2}/K_c$, whence

$$\dot{C} = (X_r/C^{3/2} + \dot{S}_a C^{1/2} T)^n \tag{11}$$

with $\dot{C} = dC/dT$ and $\dot{S}_a = dS_a/dT = S_a/T$. Noting that the initial condition for the crack now becomes $C = 1$ at $T = 0$, and the final condition $\dot{C} = 1$, the time-to-failure $T_f$ may be computed for any specified parameters $X_r$, $n$, and $S_a$. Figure 3 shows the strength $S = \dot{S}_a T_f = \sigma/\sigma_i^0$ as a function of stress rate $\dot{S}_a$, for $n = 17.9$ (see Section III) and several values of residual-stress parameter in the allowable range $0 \leq X_r \leq 1$ (corresponding to bounds set by $K_r = 0$ and $K_r = K_c$ at the initial configuration $c = c_0'$ in Eq. (1)).* It is clear that residual contact stresses can have a significant detrimental effect on the fatigue strength.

## III. Experimental Determination of Dynamic Fatigue Characteristics

### *(1) Test Procedure*

Soda-lime glass (commercial sheet) disks (nominally 50 mm in diam. by 3 mm thick) were used as test specimens. A Vickers diamond pyramid indenter was used to produce a well-defined radial crack pattern ($c > a$ (Fig. 1)) at the center of each disk. The contact itself was maintained for a standard 15 s. Two types of specimens were prepared: "as-indented" specimens ($\chi_r > 0$), using either oil (inert) or air (noninert) as contact environment; "annealed" specimens ($\chi_r = 0$), by slowly heating (over ≈1 day) air-indented disks to 520°C, holding for ≈2 days, and slowly cooling (over ≈1 day) to room temperature. Microscopic examination of the contact sites was made to check the level of birefringence associated with the residual stresses[17] and to monitor any postindentation crack development.

The disks were then loaded in center-symmetric flexure, indented face on the tension side, and taken to failure. A specially designed jig, capable of delivering a biaxial tensile stress with >99% uniformity over the inner span region, was used for this purpose.[20] With this arrangement the results were insensitive to exact positioning and orientation of the crack pattern with respect to the coaxial load axis. A microscope incorporated into the equipment provided a facility for following the progress of the radial cracks during loading. This facility was also useful for ensuring crack sharpness in annealed specimens; a preliminary stress cycle was applied to these specimens, in air environment, such that a minute amount of slow crack growth occurred. The tests proper were conducted in either oil or distilled water; for air-indented specimens a drop of the appropriate liquid was simply placed onto the contact site prior to loading (on a surface heated with a hair dryer, in the case of oil, to remove excess moisture). After placing a cover slip over the liquid, the initial crack size was recorded and the stress applied at a prescribed constant rate until failure occurred.

Figure 4 shows fracture surfaces of annealed and as-indented specimens broken in a water environment. In each case subcritical growth has expanded the median/radial crack responsible for the failure well beyond the initial indentation flaw. Noting that both specimens were subjected to identical test conditions, it is clear from the micrographs that the as-indented specimen has experienced the greater crack driving force, consistent with the existence of a tensile residual-stress component. It is also apparent from Fig. 4 that the lateral crack system is unlikely to be an influential factor in the fatigue strength; however, since the lateral and radial systems tended to comparable dimensions in the initial indentation configuration, the same conclusion cannot be extended to the inert strength.

### *(2) Inert Strengths*

Some calibration-strength runs were made under essentially equilibrium fracture conditions to evaluate the parameters within the square brackets in the fatigue relation Eq. (9). This evaluation was made for annealed and as-indented disks, with due attention in each case to the requirement that radial/lateral interactions be negligible.

With annealed disks the preliminary stress cycle used to "sharpen" the cracks in air was intensified to the extent that the characteristic dimension of the radial system exceeded that of the lateral system by at least a factor of two (recall that the lateral cracks do not respond to flexural stresses). The inert strengths $\sigma_i^0$ (oil environment) were then measured. Negligible subcritical extension of the radial crack from its initial size $c_0'$ was observed during the loading, indicating that the stress rate used (6.6 MPa s$^{-1}$) was sufficient to prevent significant penetration of moisture through the oil to the

*These calculations, based as they are on Eq. (8), do not consider the possibility of a fatigue limit or stage II and stage III crack-growth regions.

crack tip. The results, from 21 specimens indented over the load range 5 to 100 N, combine with Eq. (6) to give

$$K_c/(\pi\Omega)^{1/2}=\sigma_i{}^0 c_0{}'^{1/2}=0.78\pm0.02 \text{ MPa m}^{1/2} \quad (12)$$

With as-indented disks a different means of avoiding lateral-interaction effects had to be adopted; the need to respect the condition $c_0'<c_m$ in order for Eq. (7) to remain valid precluded the previous approach of expanding the radial crack in a pretest cycle. Instead, use was made of the observation in oil-indented surfaces that at low loads the development of the lateral system tended to lag that of the radial system to a considerable degree. For example, at $P=5$ N the lateral cracks immediately after indentation were usually so small as to be contained within the contact zone, but after $\approx 1$ h they had grown out to the limits of the radial cracks (presumably due to traces of moisture in the oil environment; during this time the radial dimension itself increased, albeit by a relatively small amount). Accordingly, by varying the interval between completion of indentation and commencement of flexural loading, the strength characteristics could be measured as a function of lateral/radial crack size. The results are plotted in Fig. 5. The zero-lateral limit, $\sigma_i{}^r P^{1/3}=115\pm5$MPa $N^{1/3}$, together with Eqs. (7) and (12), then gives

$$K_c/\chi_r=(256/27)\{[(\pi\Omega)^{1/2}/K_c](\sigma_i{}^r P^{1/3})\}^3$$
$$=31.1\pm 3.5 \text{ MPa m}^{1/2} \quad (13)$$

In these tests, significant precursor stable growth was always observed in the radial crack prior to instability, confirming the necessary existence of an energy barrier to failure.

### *(3) Dynamic Fatigue Tests*

With the dynamic fatigue tests a fixed indentation schedule was adopted for all specimens, consisting of contact in air at a peak load $P=5$ N followed by an interval of 30 min before strength testing (as-indented disks) or heat treatment (annealed disks). The contact load was chosen such that the radial crack system remained well defined at all times yet never achieved a scale requiring specimen-thickness effects to be considered as a factor in the strength analysis. This procedure conveniently afforded a consistent initial crack size, $c_0'=67\pm5$ $\mu$m, for both annealed and as-indented specimens.

Figure 6 shows the results for the two specimen preparations. The difference between the two sets of data confirms a significant residual-stress effect in the fatigue properties. In this plot the solid curve through the data points for *annealed* specimens was generated by a curve-fit procedure. First, a (logarithmic) linear fit was made in accordance with Eq. (10)* from the slope and intercept, in conjunction with the values of $c_0'$ and $K_c/(\pi\Omega)^{1/2}$ already determined, this gave the kinetic parameters $n=17.9\pm0.5$ and $v_0=2.4\pm0.6$ mm $s^{-1}$. Then substitution of these parameters, along with the appropriate conditions $\chi_r=0$ and $P=5$ N, into Eq. (9) produced a more exact evaluation (via numerical integration) of the function $\sigma^0(\dot{\sigma}_a)$, particularly at high stress rates where the strength approaches the inert limit. The curve through the data points for *as-indented* specimens was computed in a similar fashion from Eq. (9), but with $K_c/\chi_r$ in Eq. (13) substituted as appropriate to the function $\sigma^r(\dot{\sigma}_a)$. Thus, taking the results for specimens free of residual stress as a base for calibrating the crack-velocity relation Eq. (8), we have been able to predict a priori the dynamic fatigue response (to within the limits of experimental accuracy) for specimens in their natural, nonannealed state.

An additional check on the theory was made by monitoring the entire subcritical crack evolution for both annealed and as-indented disks at a particular stress rate. Figure 7 shows the data, together with the predicted $c(t)$ curves from Eq. (9). (Note that the crack does not extend noticeably immediately upon application of the stress, consistent with the expected reduction in $K_r$ due to the preceding postindentation expansion $c_0\rightarrow c_0'$.)

## IV. Discussion

The results summarized in Fig. 6 demonstrate clearly that residual contact stresses can have a significant detrimental effect on the fatigue properties of soda-lime glass. It is of interest to compare these findings with results reported in other fracture studies, particularly in regard to the value of the crack-velocity exponent $n$. In this context the present determination, $n=17.9\pm0.5$, from curve-fitting the data for annealed specimens compares favorably with the range $16<n<19$ generally obtained from macroscopic crack-velocity measurement.[21] However, if a similar force-fit procedure is conducted directly on the data for *as-indented* specimens in Fig. 6, an artificially low value, $n=13.7\pm0.2$, is measured.† A discrepancy of

*Regression analysis of ln $\sigma^0$ vs ln $\dot{\sigma}_a$. A similar fit was obtained using a more elaborate, "homologous stress ratio" technique (Ref. 6).

†The corresponding apparent velocity coefficient is $v_0=55\pm15$ ms $^{-1}$

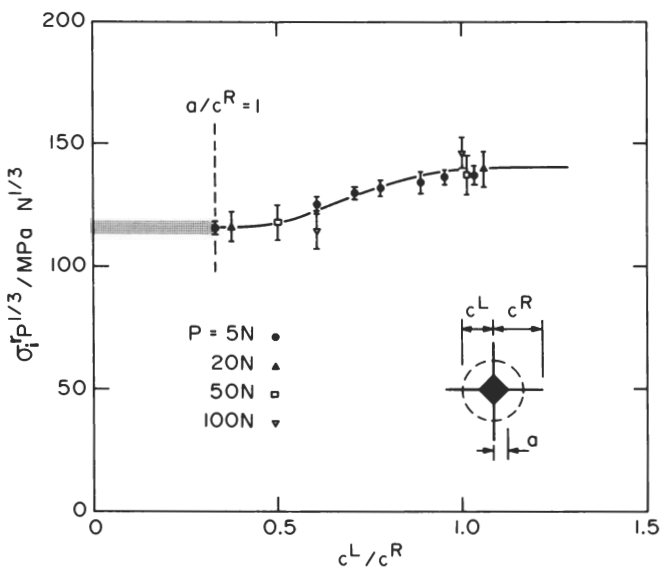


**Fig. 5.** Plot of $\sigma_i{}^r P^{1/3}$ vs lateral/radial crack-size ratio $c^L/c^R$ for specimens indented and broken in oil. Ratio $c^L/c^R$ adjusted by varying interval between contact and flexure. Shaded area represents extrapolation to $c^L/c^R\rightarrow0$ (note cracks obscured by plastic impression at $c^L<a$; dashed line designates scale of impression for $P=5$ N). Error bars are standard deviations (5–10 tests).

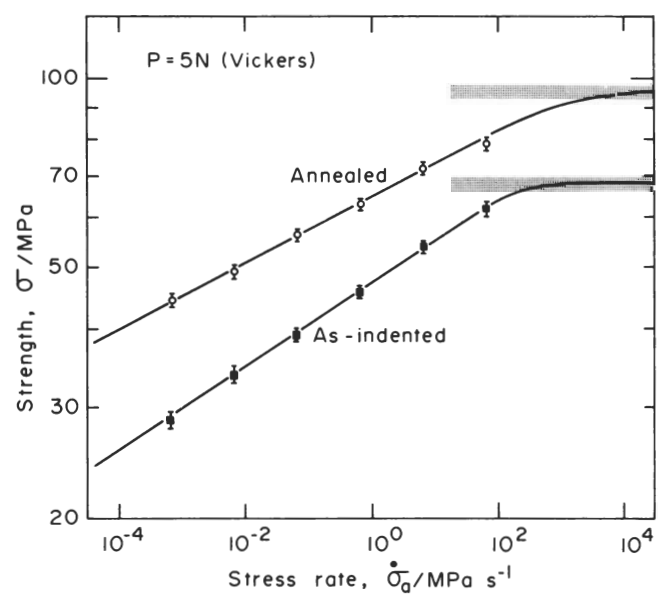


**Fig. 6.** Dynamic fatigue response for indented soda-lime glass disks broken in water. Error bars are standard deviation (10–30 specimens). Solid curve through data for specimens annealed after indentation evaluated from Eq. (9) in accordance with best fit over linear region. Solid curve through data for as-indented specimens is a priori evaluation from Eq. (9), using kinetic fracture parameters obtained in the annealed-data fit. Shaded regions indicate inert strengths, from Eq. (12) at $c_0'=67$ $\mu$m (annealed) and Eq. (13) at $P=5$ N (as-indented).

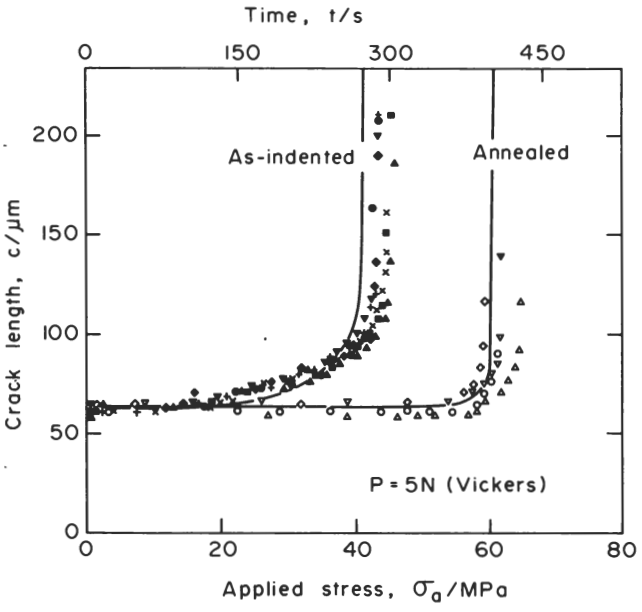


**Fig. 7.** Evolution of indentation flaws in soda-lime-glass/water system at constant applied stress rate $\dot{\sigma}_a = 0.15$ MPa·s$^{-1}$. Data for specimens annealed after contact cycle and as-indented (each symbol represents different crack). Solid curves are predictions from Eq. (9).

this magnitude was noted in an earlier dynamic fatigue study of acid-polished ($n = 16.9$) vs abraded ($n = 13.0$) specimens[7] (although in that work the experimental scatter ($\approx$25% std. dev.) cast some doubt on the significance of the difference). It is apparent that the nature and history of the controlling flaws, factors generally not considered in the basic "Griffith strength" formulation, can play an important role in the mechanics of failure. There is an implication here that certain types of flaws, particularly those associated with previous surface-contact events, respond in much the same way as the idealized "median-radial" crack system; i.e. the stress field responsible for their formation is essentially elastic/plastic in nature.

Although explicit attention has been given in this study to one material only, soda-lime glass, the residual-stress effect is expected to extend to most ceramics which exhibit fatigue. For such stresses to develop during indentation the material immediately beneath the contact point must deform radially at constant density; it is then the accommodation of the impression volume within the surrounding elastic/plastic matrix which sets up the residual field.[18] "Anomalous" (high silica content) glasses,[22] which show a tendency to deform by densification rather than by shear-induced flow, and "soft" (low hardness-to-modulus ratio) materials, which tend to flow upward around the indenter ("pile-up")[23] rather than radially outward, would therefore appear to be less susceptible to this effect. The existence of a strong residual-stress influence has indeed been demonstrated in the strength behavior of a wide range of ceramics.[19,24] Furthermore, systematic discrepancies in crack-velocity/dynamic-fatigue determinations of $n$ similar to those already described for glass have been found in materials as diverse as cement paste[9] and glass-ceramics.[12]

The results of this study therefore suggest that in-service lifetimes for brittle components should not be predicted from fracture data without due consideration of flaw characteristics. This caution is particularly valid where macroscopic-crack measurements are used to establish velocity parameters; failure to account for residual stresses in the microscopic-flaw response might then be expected to lead to substantial inaccuracy in the lifetime calculation. If, on the other hand, the parameter calibration is obtained exclusively from dynamic fatigue data on the actual component surfaces, via Eq. (10), much of this inaccuracy may be inadvertently eliminated; this can be argued on the reasonable assertion that static and dynamic fatigue relations are likely to be similarly affected by any modifications in the flaw micromechanics. There would appear to be a need for further investigation into the general area of flaw characterization in the design of strong ceramics.

**Acknowledgments:** The writers thank M. V. Swain and P. Chantikul for helpful discussions on aspects of this work and P. Kelly for technical assistance.

## References

[1] S. M. Wiederhorn; pp. 613–46 in Fracture Mechanics of Ceramics, Vol. 2. Edited by R. C. Bradt, D. P. H. Hasselman, and F. F. Lange. Plenum, New York, 1974.
[2] A. G. Evans and S. M. Wiederhorn, "Proof Testing of Ceramic Materials. An Analytical Basis for Failure Prediction," *Int. J. Fract.*, **10** [3] 379–92 (1974).
[3] S. M. Wiederhorn; pp. 635–65 in Ceramics for High Performance Applications. Edited by J. J. Burke, A. E. Gorum, and R. N. Katz. Brook Hill, Chestnut Hill, Mass., 1974.
[4] A. G. Evans and H. Johnson, "The Fracture Stress and its Dependence on Slow Crack Growth," *J. Mater. Sci.*, **10** [2] 214–22 (1975).
[5] J. E. Ritter, Jr.; pp. 667–86 in Fracture Mechanics of Ceramics, Vol. 4. Edited by R. C. Bradt, D. P. H. Hasselman, and F. F. Lange. Plenum, New York, 1978.
[6] K. Jakus, D. C. Coyne, and J. E. Ritter, Jr., "Analysis of Fatigue Data for Lifetime Predictions for Ceramic Materials," *J. Mater. Sci.*, **13** [10] 2071–80 (1978).
[7] J. E. Ritter, Jr. and R. P. LaPorte, "Effect of Test Environment on Stress-Corrosion Susceptibility of Glass," *J. Am. Ceram. Soc.*, **58** [7–8] 265–67 (1975).
[8] J. E. Ritter, Jr. and K. Jakus, "Applicability of Crack Velocity Data to Lifetime Predictions for Fused Silica Fibers," *ibid.*, **60** [3–4] 171 (1977).
[9] S. Mindess and J. S. Nadeau, "Effect of Loading Rate on the Flexural Strength of Cement and Mortar," *Am. Ceram. Soc. Bull.*, **56** [4] 429–30 (1977).
[10] H. C. Chandan, R. C. Bradt, and G. E. Rindone, "Dynamic Fatigue of Float Glass," *J. Am. Ceram. Soc.*, **61** [5–6] 207–10 (1978).
[11] B. J. Pletka and S. M. Wiederhorn; pp. 745–59 in Ref. 5.
[12] B. R. Lawn and T. R. Wilshaw, "Indentation Fracture: Principles and Applications," *J. Mater. Sci.*, **10** [6] 1049–81 (1975).
[13] B. R. Lawn and E. R. Fuller, "Equilibrium Penny-Like Cracks in Indentation Fracture," *ibid.*, [12] 2016–24.
[14] B. R. Lawn and A. G. Evans, "A Model for Crack Initiation in Elastic/Plastic Indentation Fields," *ibid.*, **12** [11] 2195–99 (1977).
[15] B. R. Lawn and D. B. Marshall, "Residual Stress Effects in Failure From Flaws," *J. Am. Ceram. Soc.*, **62** [1–2] 106–108 (1979).
[16] B. R. Lawn and D. B. Marshall, "Hardness, Toughness, and Brittleness: An Indentation Analysis," *ibid.*, [7–8] 347–50.
[17](*a*) D. B. Marshall and B. R. Lawn, "Residual Stress Effects in Sharp Contact Cracking: I," *J. Mater. Sci.*, **14** [8] 2001–12 (1979).
(*b*) D. B. Marshall, B. R. Lawn, and P. Chantikul, "Residual Stress Effects in Sharp Contact Cracking: II," *ibid.*, [9] 2225–35.
[18] B. R. Lawn, A. G. Evans, and D. B. Marshall, "Elastic/Plastic Indentation Damage in Ceramics: The Median/Radial Crack System"; this issue, pp. 574–81.
[19] J. J. Petrovic and M. G. Mendiratta; pp. 83–102 in Fracture Mechanics Applied to Brittle Materials. Edited by S. W. Freiman. *ASTM Spec. Tech. Publ.*, No. **678**, 1979.
[20] D. B. Marshall, "An Improved Biaxial Flexure Test for Ceramics," *Am. Ceram. Soc. Bull.*, **59** [5] 551–53 (1980).
[21] S. M. Wiederhorn; unpublished work.
[22] A. Arora, D. B. Marshall, B. R. Lawn, and M. V. Swain, "Indentation Deformation/Fracture of Normal and Anomalous Glasses," *J. Non-Cryst. Solids*, **31** [3] 415–28 (1979).
[23] D. Tabor, Hardness of Metals. Clarendon, Oxford, England, 1951.
[24] P. Chantikul, G. R. Anstis, B. R. Lawn, and D. B. Marshall; unpublished work.